

## Investigation of salt plugs intrusion into Dehnow anticline using image processing and geophysical magnetotelluric methods

A. Esmail Zadeh,<sup>1</sup> F. Doulati Ardejani,<sup>1</sup> M. Ziiai,<sup>1</sup> and M. Mohammado Khorasani<sup>2</sup>

Received 28 December 2009; accepted 22 January 2010; published 5 March 2010.

This paper attempts to consider the results of a magnetotelluric (MT) geophysical survey and the applicability of image processing method on the TM images of the anticline. The color pixels related to the salt zones have been separated from the other zones from the land surface using image processing method incorporating *k*-means clustering approach as one of the simplest unsupervised learning algorithms. Field investigations, geological study and the results obtained from the MT survey together with the image processing method identified three salt zones in the study area. These salt zones match well with a decrease in the resistivity of MT data. The application of the proposed method as one of the artificial intelligence technique can be properly used as a cost effective method to identify salt zones from the other areas and preparing a probability map in a regional scale in petroleum exploration. **KEYWORDS:** *Magnetotelluric; Dehnow anticline; salt plug; image processing; color pixels; cluster.*

**Citation:** Esmail Zadeh, A., F. Doulati Ardejani, M. Ziiai, and M. Mohammado Khorasani (2010), Investigation of salt plugs intrusion into Dehnow anticline using image processing and geophysical magnetotelluric methods, *Russ. J. Earth. Sci.*, 11, ES3008, doi:10.2205/2009ES000375.

### Introduction

From geological point of view, Dehnow area is a part of the Fars sedimentary basin in south-east Iran. The evidences of the salt outcrops can be recognized at two points from Dehnow anticline. The detailed geological investigations in the area proved the presence of two series of perpendicular faults. The first type of the faults with NW–SE direction may be formed oil seeps due to the extension of these types of faults to the dipper layers. Furthermore, the second types of faults in the salt layers of the Hormoz formation at the base of the Dehnow anticline can be related to the salt intrusion.

A basic study of the geology of the area, a detail investigation of structural features such as faults associated with the Dehnow anticline and application of the geophysical tech-

niques and other exploration methods is necessary to investigate the subsurface extension of the this anticline and to identify salt plug intrusion into the anticline. Furthermore, the information obtained by the various exploration techniques help in the design of a cost management program relating to any further investigation in the area.

Magnetotelluric (MT) geophysical method has been recently used in many applications relating to petroleum exploration studies as a way of investigating dip extension of oil traps and exploring the impact of faults and intrusions into such geological structures [Oskooi, 2004].

Furthermore, the image processing technique may be used to accurately explore the geological features under local maps but the image segmentation is a classic inverse problem which consists of achieving a compact region-based description of the image scene by decomposing it into meaningful or spatially coherent regions sharing similar attributes. This low-level vision task is often the preliminary (and also crucial) step in many video and computer vision applications, such as object localization or recognition, data compression, tracking, image retrieval, or understanding. Because of its simplicity and efficiency, clustering approaches were one of the first techniques used for the segmentation of (textured) the natural images [Banks, 1990; Zimmerman, 1991].

<sup>1</sup>Faculty of Mining, Petroleum and Geophysics, Shahrood University of Technology, Shahrood, Iran

<sup>2</sup>National Iranian Oil Company, Exploration Department, Tehran, Iran

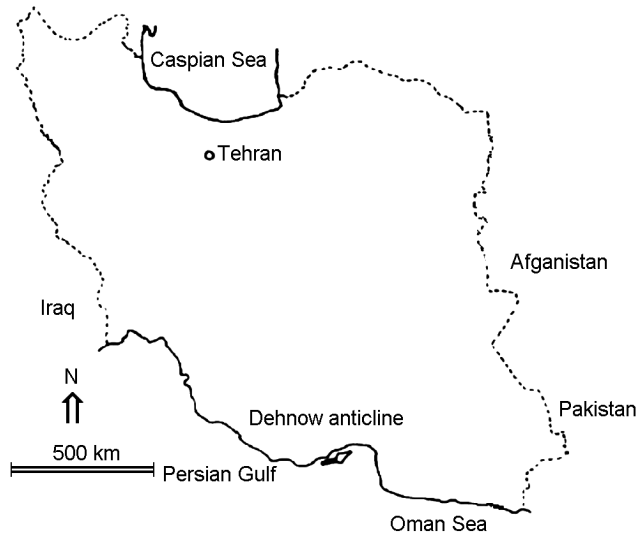


**Figure 1.** Geographical situation of Dehnow anticline, south-east Iran.

The literature review has shown that despite many research works have been done to investigate the applicability of the MT method and image processing analysis related to earth sciences and mining industry [Esmail Zadeh et al., 2009], the applications of these methods associated with petroleum exploration and related researches have not been widely reported so far. The main objective of the present study was to identify the dip extension of the Dehnow anticline and to detect any intrusive mass, faults and salt plugs using MT data and image processing technique. It should

be noted that a salt outcrop can be easily seen at the east part of the anticline. This may be an important evidence showing salt plug intrusion in the area.

### Geographical Location

Dehnow area is between latitudes 27°1' and 27°14' and longitudes 53°35' and 53°59' (Figure 1). The study area is surrounded by Ashkenan, Ahal, Boochir, Hamiran, Hashniz and Kemeshck cities. Tabnack gas structure is located in the west of this district. The area can be accessed through Asalouie–Bandarlengeh and Lamard–Ashkenan–Gavbandy roads. The area has a very harsh topography with mountains and valleys. The climate of the area is very hot and wet in the summer and an average climate condition in the winter.

### Geological Settings

Dehnow area is a part of the Fars sedimentary basin at south-east Iran. Khamy formation and Bangestan group are the oldest geological structures in the area that have outcrops. Younger structures consist of Aghajary, Mokhtari, Mishan, Gachsaran and Asmary. Dominant structural trend in the area is northwest–southeast. Dehnow anticline is located between Hendurabi and Razak faults. These faults are almost perpendicular to the Dehnow anticline. Taking the combined geological-residual gravity contour map into account (Figure 2), a northwest-southeast trend can be con-

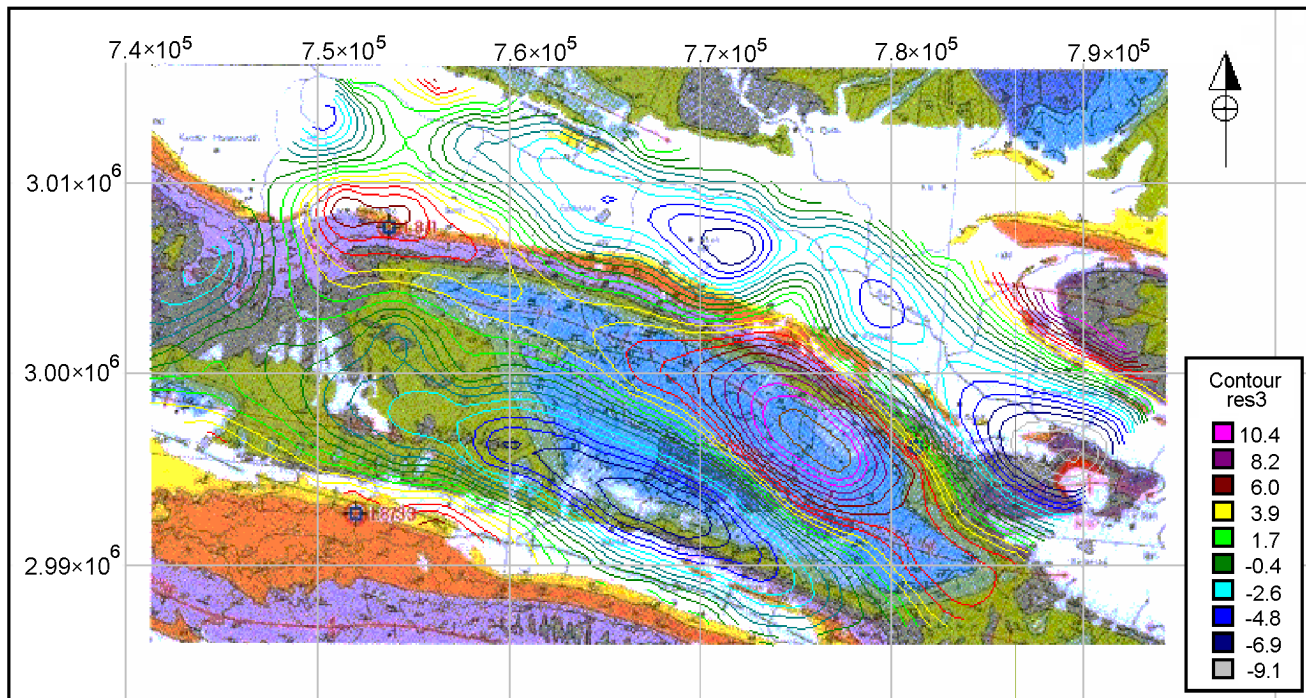


**Figure 2.** Combined geological-residual gravity map of the study area [Doulati Ardejani, 2005].

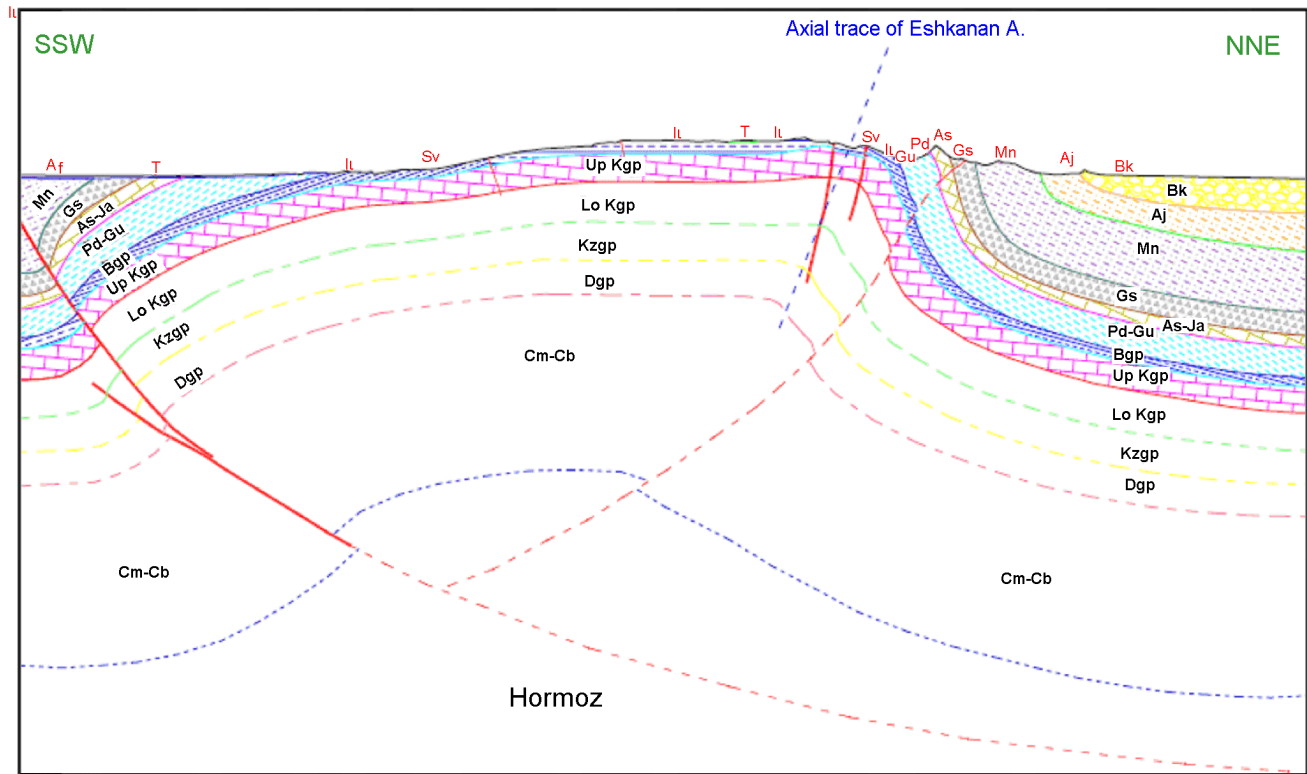


**Figure 3.** Structural geology section of the Dehnow anticline. This illustrates Hormoz salt intrusion [Genevraye *et al.*, 1976, modified after Bagheri, 2005]

sidered for the Dehnow anticline. A low gravity anomaly fits well the salt outcrop in the south-east of the anticline.

Although not presented here, the structural geology investigations have shown that the folding system of the anticline has been affected by Hormos Salt formation. This even caused an outcrop of the salt at the south-east of the anticline [Bagheri, 2005]. Figure 3 shows a structural geology section of the Dehnow anticline; illustrating Hormoz salt intrusion [Genevraye *et al.*, 1976, modified after Bagheri, 2005].

## Materials and Methods

Magnetotelluric (MT) is one of the geophysical methods that can be used for dip investigations in petroleum exploration. In MT method, the natural electromagnetic fields of earth are used to investigate the electrical conductivity of the geological layers of the Earth. The relationship of amplitude, phase and direction between electric ( $E$ ) and magnetic ( $H$  or  $B$ ) fields depend on the distribution of the electrical conductivity of the subsurface bodies. Equations 1 and 2 can be used to calculate the resistivity of the structures at different depths by taking the measured values of  $E$  and  $H$  in different directions into consideration:

$$E_x(f) = H_{xx}(f)H_x(f) + Z_{xy}(f)H_y(f) \quad (1)$$

$$E_y(f) = Z_{yx}(f)H_x(f) + Z_{yy}(f)H_y(f) \quad (2)$$

Such relationships, calculated models and field measurements provide useful information for the regions of interest within the earth from depths of a few tens of meters to the upper mantle [Vozoff and Nabighian, 1991].

MT method is normally categorized into different methods including RMT (with a frequency range of 12–240 kHz), MT method in which the frequency varies between  $10^{-4}$  and  $10^{-3}$  Hz, and CSAMT (with a frequency range of  $10 - 10^4$  kHz).

These methods have been manipulated based on the electromagnetic (EM) fields of the earth. All five components of MT are required to be measured either in land or airborne for different MT methods. RMT is often used for shallow depths (about a few hundreds meters) whereas CSAMT and MT can be applied for deeper investigations (deeper than 10 kilometers) [Oskoei, 2004].

A MT survey incorporating 37 stations along 3 profiles has been performed at the study area by the Geosystem Company [Tabatabai, 2005]. Two profiles are selected on the Dehnow anticline, almost perpendicular to its axis, with a measuring spacing of 1000–2000 m. The third profile is at the south of the anticline wherein a salt plug has outcrop. The MT data were measured along this profile with a spacing of 500–600 m. This profile was observed on the salt outcrop in order to calibrate the MT instrument with the region. The MT data have been initially processed and interpreted by the Geosystem Company. In this paper, the results of

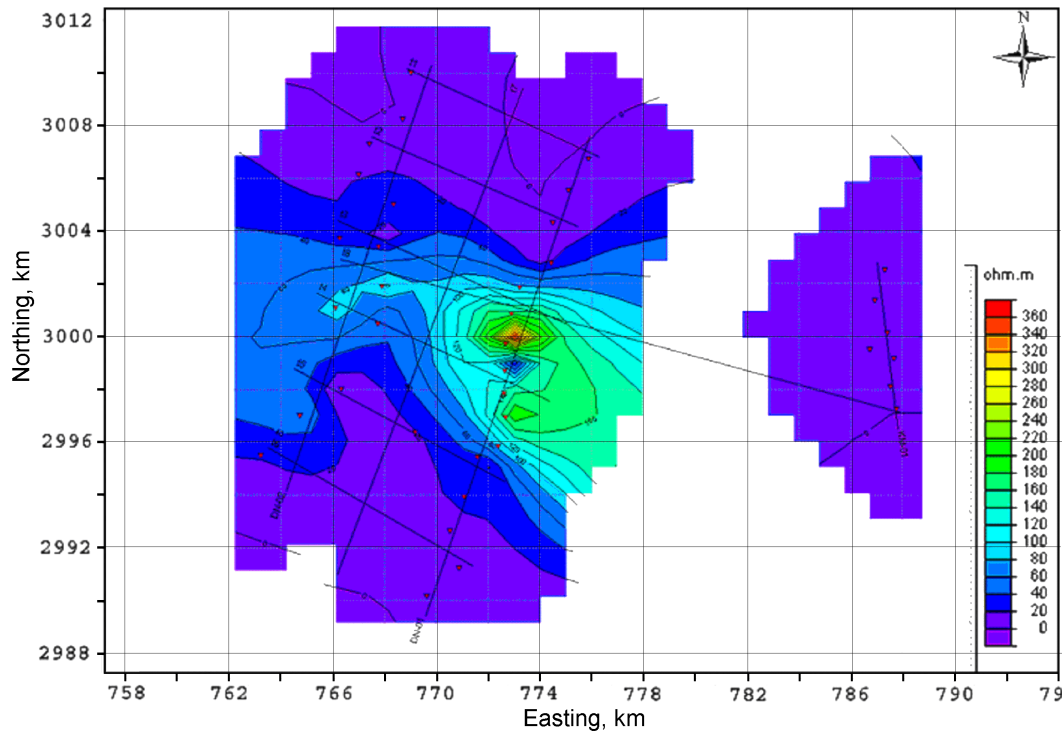


Figure 4. Resistivity contour map for depth of 500 m.

the processing have been inversely modeled and interpreted by a commercial computer-based software called Winglink (Geosystem Company, 2008, Winglink, a multidisciplinary software program to process, interpret and integrate several geophysical disciplines in a unique interpretation model. Available online at: <http://www.geosystem.net/how.html>, accessed September 2008).

Color design always plays an important role in visual art, industrial design, and image processing. The clustering process can be organized in different color spaces. Among color spaces a special role plays the CIELAB color space. The CIELAB color space (also known as  $L^*a^*b^*$  or  $CIE\ L^*a^*b^*$ ) is derived from the CIE  $XYZ$  tristimulus values. The CIELAB space consists of a luminosity layer  $L^*$ , chromaticity-layer  $a^*$  indicating where color falls along the red-green axis, and chromaticity-layer  $b^*$  indicating where the color falls along the blue-yellow axis. The  $L$  axis ranges from 0 to 100, the  $a$  and  $b$  axes both range from  $-128$  to  $128$ . All of the color information is in the  $a^*$  and  $b^*$  layers. Since the color information exists in the  $a^*b^*$  space and objects are pixels with  $a^*$  and  $b^*$  values. It can be measured the difference between two colors using the Euclidean distance metric as objective function. But one of the most problems in clustering remote sensing image is to separate dark color from light color in a cluster. We use the  $L^*$  layer contains the brightness value of each color for extracting the brightness values of the pixels in a cluster from darkness values [Quan et al., 2009].

After the selection and the extraction of the image features (usually based on color and/or texture and computed on (possibly) overlapping small windows centered around the pixel to be classified), the feature samples, handled as vectors, are grouped together in compact but well-separated clusters corresponding to each class of the image. The set of connected pixels belonging to each estimated class thus defined the different regions of the scene. The method recognized as  $K$ -means cluster [Lloyd, 1982] (and its fuzzy version called fuzzy  $C$ -means) are some of the most commonly used techniques in the clustering-based segmentation field [Berkhin, 2002]. A cluster is a collection of data objects that are similar to one another with in the same cluster and are dissimilar to the objects in the other clusters. It is the best suited for mining data because of its efficiency in processing large data sets.  $K$ -means is one of the simplest unsupervised learning algorithms that solve the well known clustering problems. The procedure follows a simple and easy way to classify a given data set through a certain number of clusters (assume  $k$  clusters) fixed a priori. The main idea is to define  $k$ -centroids, one for each cluster. These centroids should be placed in a cunning way because of different location causes different result. So, the better choice is to place them as much as possible far away from each other. The next step is to take each point belonging to a given data set and associate it to the nearest centroid. When no point is pending, the first step is completed and an early

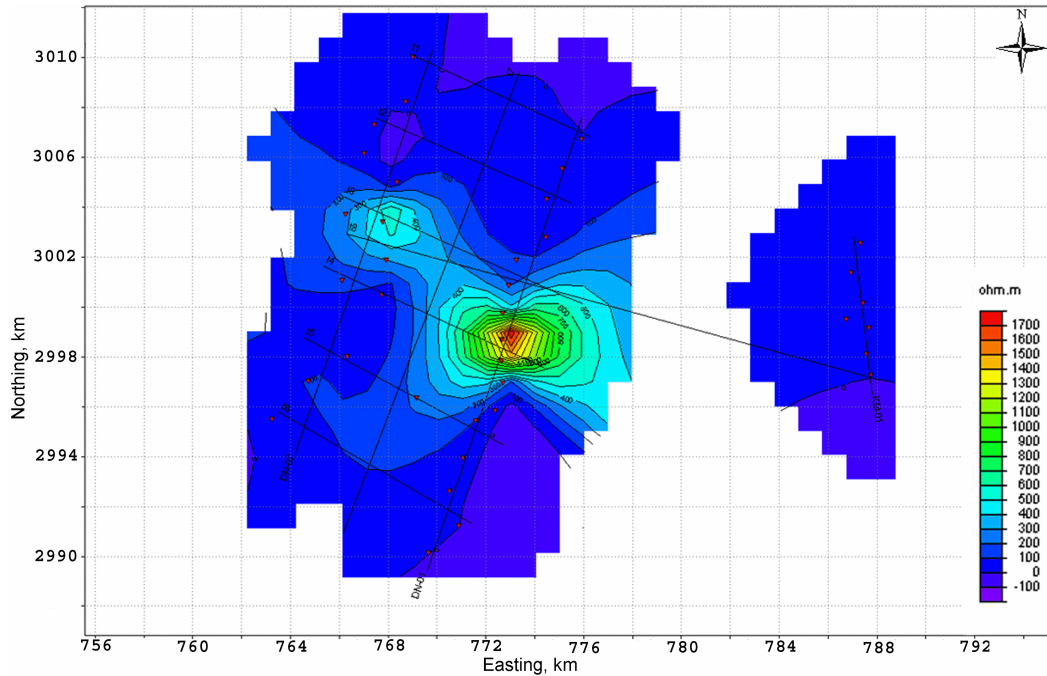


Figure 5. Resistivity contour map for depth of 1000 m.

groupage is done. At this point we need to re-calculate  $k$  new centroids as barycenters of the clusters resulting from the previous step. After we have these  $k$  new centroids, a new binding has to be done between the same data set points and the nearest new centroid. A loop has been generated. As a result of this loop we may notice that the  $k$  centroids change their locations step by step until no more changes are achieved. In other words, centroids do not move any more [Maheswary and Srivastav, 2008]. The algorithm is composed of the following steps:

- (1) Initialize  $K$  as the number of clustering;
- (2) Assign every node to the nearest clustering according to a given distance;
- (3) Calculate the new clustering center;
- (4) Repeat steps (2) and (3) until the cluster center did not change anymore.

For the given  $n$ -dimension data set  $D\{D_1, D_2, \dots, D_t\}$ , we initialized  $K$  and randomly chose  $K$  nodes in  $D$  as initial cluster centers, and defined  $d(D_i, D_j)$  as the distance between data vectors  $D_i$  and  $D_j$ .

## Results and Discussions

### MT Results

A computer software called Winglink has been used to interpret the MT data when the necessary corrections and processing have been made on the measured data. The re-

sistivity sections were selected in different directions on MT map in order to have a better comparison the results. Resistivity contour maps were then produced for different depths of 500, 750, 1000, 1250, 1500, 1750 and 2000 m (Figure 4, Figure 5, Figure 6, and Figure 7).

As well illustrated in Figures 4–7, the resistivity increased with depth. The higher resistivity can be associated to the basement rocks. The reduction in resistivity at the eastern part of the anticline can be related to the salt plug intrusion emanated from the Hormoz formation.

As Figure 6 shows, reduction in the resistivity at the eastern part of the anticline is more obvious in the map produced for depth of 1500 m due to the salt plug intrusion. This can be also seen in Figure 6 plotted for the resistivity of depth of 2000 m. The high resistivity of the rocks in the central part of the area can be related to the basement.

Comparison of Figures 4–7 shows that the central part of the Dehnow anticline was ruptured. This happened in the position of the Profile  $t7$  due to a dip fault that affected the resistivity data. This fault can be even recognised from the land surface.

### Image Processing Results

Image processing investigated in the present research is limited within  $27^\circ 1'$  and  $27^\circ 14'$  N latitudes and  $53^\circ 35'$  and  $53^\circ 59'$  longitudes from Landsat TM imagery acquired in 2000. ENVI as the image pre-processing software was used. The  $K$ -mean algorithm and clustering method under TM image was also used to identify salt plug intrusion into Dehnow

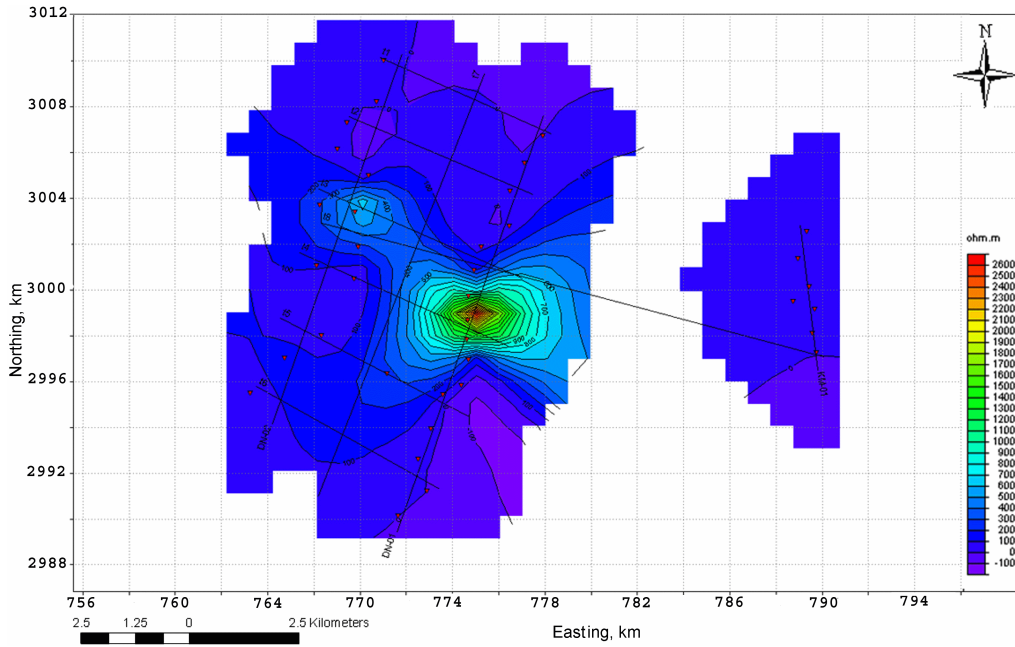


Figure 6. Resistivity contour map for depth of 1500 m.

anticline. In this study, RGB values translated into the CIELAB color model. The interested areas have been recognized from a set of 5 clusters produced by the image processing analysis on the TM image of Dehnow area.

This system is implemented using MATLAB image processing tools and statistical tools.

Figure 8 shows the TM image of the Dehnow anticline in which the gravity and magnetic profiles are also illustrated.

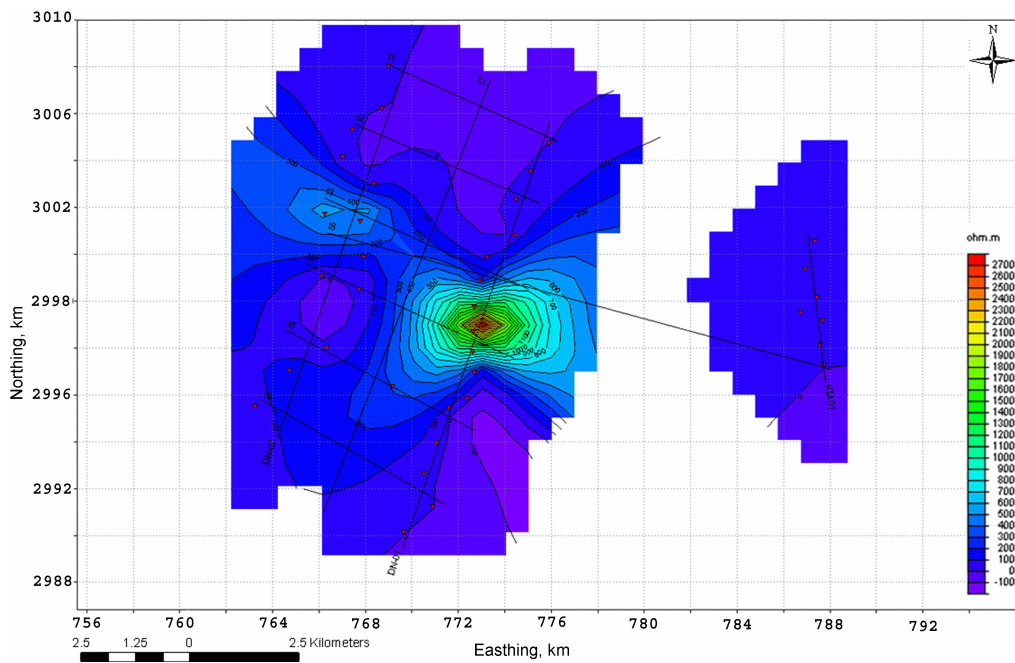


Figure 7. Resistivity contour map for depth of 2000 m.

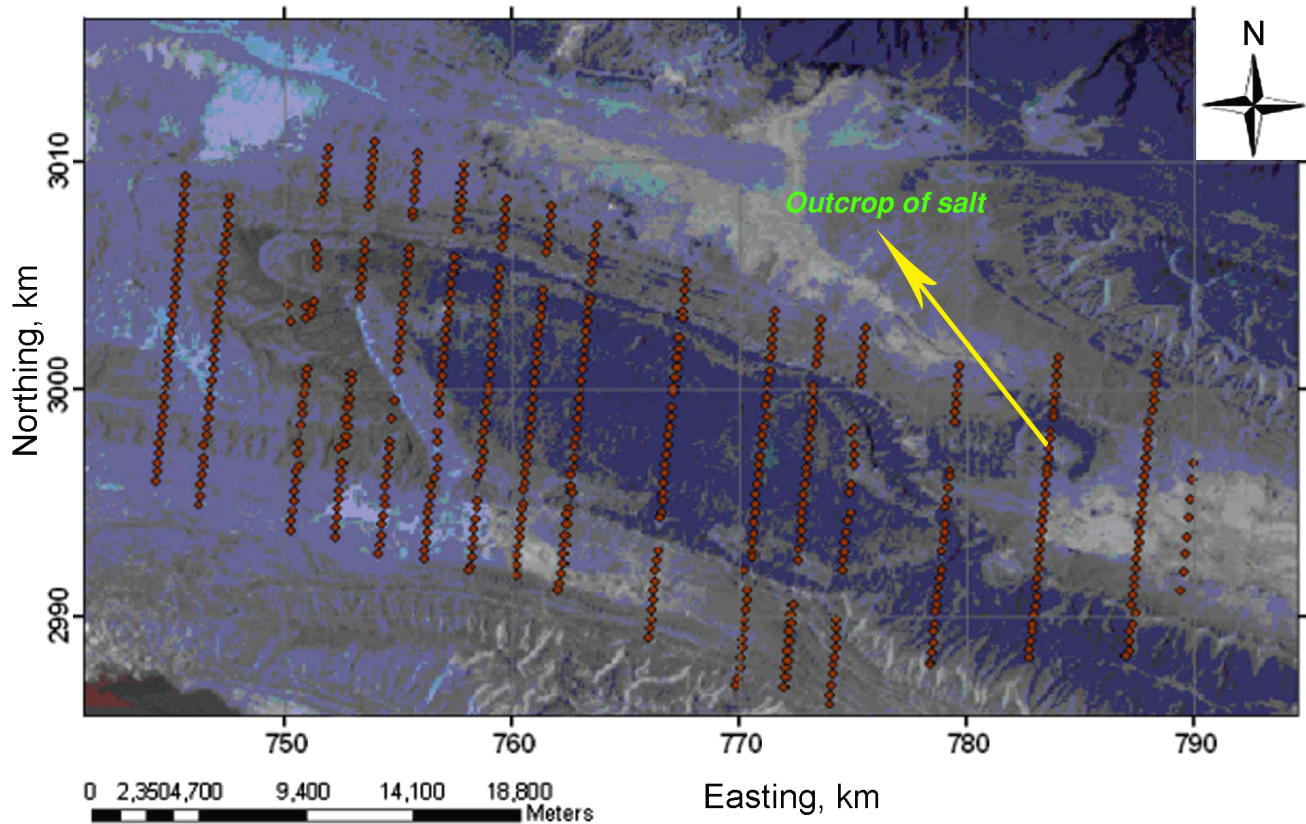


Figure 8. TM image of the Dehnow anticline including gravity and magnetic profiles and stations.

An outcrop of salt is well illustrated at south-east of the Dehnow anticline. According to the salt outcrop in the area, the cluster 4 (Figure 9) was obtained to be the appropriate cluster for the study area. The result obtained by the cluster 4 confirms the MT results that have shown low resistivity at the east part of the Dehnow anticline. Field investigations are also agreed well with MT and image processing methods. Except the salt outcrop, two other salt areas were also predicted in Figure 9; shown as salt area 1 at the southeast of the anticline and salt area 2 at the north and northeast of the anticline. The salt area 1 conforms well to the low resistivity area at the east part of the Dehnow area as interpreted in MT maps. Field investigations have proved the presence of this salt area. Furthermore, the MT results determined a shallow depth for this salt zone. From shallow depths to depth of 1500 m, the resistivity increased. Below this depth, the resistivity decreased due to the Hormoz salt formation. The salt area 2 can not be seen at the land surface. Moreover, the resistivity is low in this area. This low resistivity zone may be related to the alluvial sediments.

## Conclusion

Although many exploration methods including detailed geological and structural geology investigations, gravity,

magnetic and seismic geophysical methods have been extensively used to study Dehnow anticline, however, the interpretation of the results could not provide useful data to detect the subsurface extension of this article and to identify any salt plug intrusion into this trap. This paper attempts to present a simple and cost-effective method to identify the dip extension of the Dehnow anticline at south-east Iran, and to detect any intrusive mass, faults and salt plugs using MT data and image processing technique. A computer software called Winglink has been used to interpret the MT data. Resistivity contour maps were produced for different depths of 500, 750, 1000, 1250, 1500, 1750 and 2000 m. The results obtained from the MT method shows that resistivity increased with depth. The higher resistivity can be associated with the basement rocks. The reduction in the resistivity at the south-east of the anticline can be related to the salt plug intrusion emanated from the Hormoz formation. Furthermore, the results of the image processing technique incorporating *K*-mean algorithm and clustering method under TM image show that the cluster 4 was the appropriate cluster for the study area according to the salt outcrop at the east part of the Dehnow anticline. The result obtained by the cluster 4 confirms the MT results that have shown low resistivity at the east part of the Dehnow anticline. Field investigations are agreed well with MT and image processing methods. Except the salt outcrop, two other salt areas were also predicted by the image processing method. These are salt area 1 at

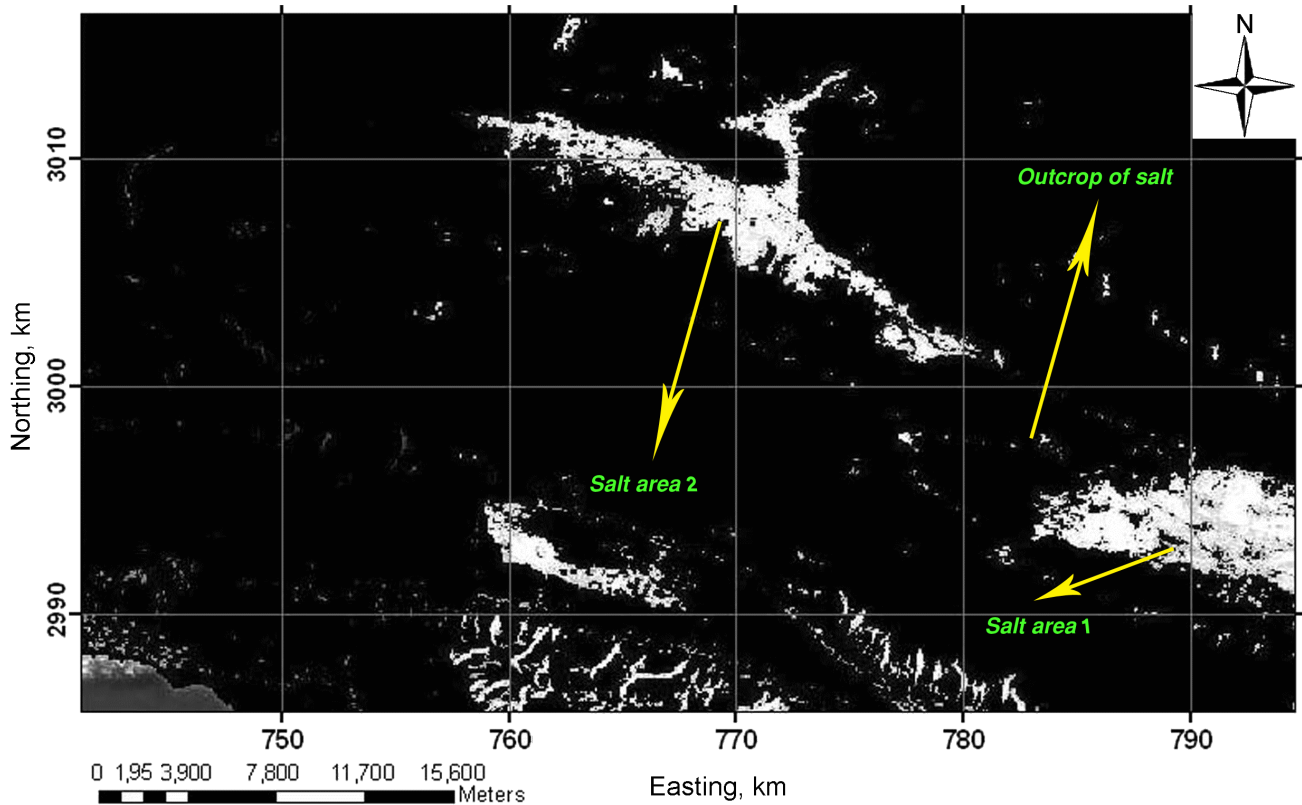


Figure 9. The result of image processing analysis for cluster 4.

the southeast of the anticline and salt area 2 at the north and northeast of the anticline. The salt area 1 with a low resistivity can be recognised by the field investigations. The MT results determined a shallow depth for this salt zone. From shallow depths to depth of 1500 m, the resistivity increased. Below this depth, the resistivity decreased due to the Hormoz salt formation. The salt area 2 can not be seen at the land surface. Moreover, the resistivity is low in this area. This low resistivity zone may be related to the alluvial sediments.

**Acknowledgments.** The authors are grateful to National Iranian Oil Company (NIOC) for providing Winglink software.

## References

- Bagheri, J. (2005), Geometry and Kinematic Analysis of Dehnow anticline and related subsurface transverse faults (Costal Fars), *MS.c. thesis*, Department of Geology, School of Science, Tarbiat Modarres University.
- Banks, S. (1990), *Signal Processing, Image Processing and Pattern Recognition*, Prentice-Hall, Englewood Cliffs, NJ.
- Berkhin, P. (2002), *Survey of clustering data mining techniques*, Accrue Software, San Jose, CA.
- Doulati Ardejani, F. (2005), *Interpretation of the gravity and magnetic data of Dehnow anticline. Technical Report*, National Iranian Oil Company, Tehran, Iran.
- Esmail Zadeh, A., M. Ziiai, F. Doulati Ardejani (2009), Application of image processing method for exploration of oil and gas in south-west Iran, *International Conference on Electronic geophysical Year: State of the Art and Results, 3-6 June 2009, Pereslavl-Zalessky, Russia, 24*, GC RAS, Moscow.
- Genevraye, P., M. Seguret, S. Nikpour, C. Mouille, R. Perrier, P. Ahmadnia (1976), *Denhow and Namaki geological survey, Report No.5517-9-1*, Total Iran Petroleum Co., Iran.
- Lloyd, S. P. (1982), Least squares quantization in PCM, *IEEE Trans. Inf. Theory, IT-28(2)*, 129-136. doi:10.1109/TIT.1982.1056489
- Maheswary, P., N. Srivastav (2008), Retrieving Similar Image Using Color Moment Feature Detector and K-means Clustering of Remote Sensing Images, *International Conference on Computer and Electrical Engineering*, 821-824, IEEE Press, NY. doi:10.1109/ICCEE.2008.114
- Oskoi, B. (2004), A broad view on the interpretation of electromagnetic data (VLF, RMT, CSAMT), *PhD thesis*, Uppsala University, Uppsala, Sweden.
- Quan, Z., G. Zhenyu, M. Xinguo (2009), A Modified Color Appearance Model of CIELAB, *International Asia Conference on Informatics in Control, Automation and Robotics*, 339-344, IEEE Press, NY.
- Tabatabaei, Raesi (2004), Interpretation of the gravity, magnetic and magnetotelluric data of Dehnow anticline, Techni-

cal Report, *Report No.: 2083*, National Iranian Oil Company, Tehran, Iran.

Vozoff, K., M. C. Nabighian, Eds., (1991), *Electromagnetic Methods in Applied Geophysics, Vol. 2: Application, Part B*, Society of Exploration Geophysics, Tulsa.

Zimmerman, H. J. (1991), *Fuzzy Set Theory and Its Application, 2-nd Edition*, Kluwer Academic Publisher, Dordrecht.

\_\_\_\_\_

F. Doulati Ardejani, A. Esmail Zadeh, M. Ziiai, Faculty of Mining, Petroleum and Geophysics, Shahrood University of Technology, Shahrood, Iran, P.O.Box: 36155-316.  
(mziiai@shahroodut.ac.ir)

Mohammado Khorasani M., National Iranian Oil Company, Exploration Department, Tehran, Iran